Journal of Administrative and Economic Sciences • Vol 16, Issue 2 (2023) • p 61-84

Sequential Forecasting Strategies for Crypto Portfolio Allocation: A Dynamic Latent Factor Analysis Approach

Mohamed Saidane
Department of Management Information Systems and Production Management
College of Business and Economics, Qassim University
P.O. Box 6666 - Buraidah: 51452 • kingdom of Saudi Arabia
M.Saidane@qu.edu.sa

(Received: September 18, 2022 • Revised: October 30, 2022 • Accepted: November 13, 2022)

Abstract:

In this article, a highly flexible and fast framework for estimating and exploring the dynamic latent dependencies among main cryptocurrency log-returns is introduced. Our approach is inspired by latent factor analysis models capturing simultaneously the persistence of volatility clustering and the presence of leverage effect in the crypto market.

A recursive quasi-maximum likelihood strategy is proposed to infer the latent cross-sectional correlation structure of the data and then to estimate the parameters of the model. Our algorithm consists of recursively alternating between Kalman filtering and smoothing recursions and the expectation maximization (EM) algorithm. This produces economically interpretable estimates for the common latent factors, which can be used to predict the mean return vector and the return covariance matrix, particularly useful for stock selection and portfolio allocation problems.

To illustrate the performance of our sequential strategy, the model is applied to daily log-returns of the last 5 years of the Bitcoin, Ethereum, Litecoin, Monero, Binance Coin and Waves currencies. The out-of-sample forecast encompassing tests show that the factorial approach yields better forecasts than those given by typical benchmarks. In terms of cumulative financial returns, our framework seems to provide the best performing mean-variance portfolio.

Keywords: Asset allocation, Cryptocurrencies, Heteroskedastic factor analysis, EM Algorithm, Kalman Filter, Sequential forecasting.

JEL Classification codes: C32 ; C38; C53; C58.

1. Introduction

Optimal portfolio allocation has received considerable attention from practitioners and academics for a long time. The standard approach is to find the optimal distribution of resources by minimizing the risk for a given level of expected return. The major theoretical work to generate optimal portfolios through a quadratic programming procedure is due to Markowitz (1959). This theory involves generally a mean parameter and a covariance matrix of the returns which are usually estimated based on historical data. From the market risk point of view, Saidane (2017, 2019, 2022a,b) and Mosbahi et al., (2017) implemented portfolio rules in conjunction with a variety of latent factor models to accurately assess the Value-at-Risk (VaR) for the Tunisian government debt portfolio. The major results show that, during financial crisis periods, the factorial-based approach offers a good fit for the returns series of the exchange rate and gives good estimations of the VaR. From a Bayesian perspective, Putnam and Quintana (1994) and Quintana and Putnam (1996) implemented different portfolio strategies for fixed income securities and futures contracts in equity index and currency markets respectively. They use the predictive variance-covariance matrices calculated with discount methods to find the optimal portfolios.

The methodology in this paper is based on latent factor time-varying volatility models and is developed in the context of cryptocurrency market. For the inference of the latent correlation structure, we have implemented in a first time a modified version of the Kalman filter to obtain the best-filtered estimates of the common factors. Then, we used the Expectation-Maximization (EM) algorithm for the parameter's estimation. From a statistical perspective, our estimation strategy seems to be intuitive, reliable and numerically efficient.

Based on these models, we developed a sequential nonlinear forecasting strategy to predict the time-varying covariance matrices of the different crypto portfolios. The predicted mean return vectors and return covariance matrices are then used to obtain the optimal allocations of each cryptocurrency inside the portfolio. For model comparisons, we used out-of-sample predictions obtained from other alternative models - such as the simpler, widely used, dynamic variance-matrix discounting method (Aguilar and West, 2000); the naïve forecasting method based on the historical average of the available data; the mixture of probabilistic factor analyzers (Mosbahi et al., 2017) and the Gaussian state-space model (Saidane, 2006).

The rest of this paper is structured as follows. In section 2, we provide more concise formulations for the latent factor time-varying volatility model. A detailed state space-based inferential procedure for the latent factors structure is also given. Then, we present our EM algorithm to estimate the model's parameters and the latent state variables. The accuracy of our proposed sequential forecasting approach will be evaluated against the most competitive benchmarks in section 3. Then we discuss in section 4 the performance of the different sequential allocation strategies using cryptocurrency data. Finally, we conclude the paper with some final remarks and suggest the directions of the possible future research.

2. The Latent Factor Volatility Model

The model we consider throughout this paper is a dynamic generalization of the discrete-time standard factor analysis model. In this specification, we denote the price of the k-th asset in the portfolio at time t by p_{kt}.[1] For each $t = 1, \dots, T$, we compute the log-return of the different assets $r_{kt} = \log(p_{kt}/p_{kt-1})$ for all $k = 1, \dots, p$. Then, we assume a linear relationship between the log-returns and a small number of q latent factors. This framework, called discrete-time latent factor volatility model (LFVM), is defined by:

$$r_t = \Gamma z_t + \nu_t, \quad (1)$$

where r_t is the $(p \times 1)$ log-return vector of the crypto portfolio at time t, Γ denotes the $(p \times q)$ matrix of factor loadings (called also the pattern matrix) and z_t, the q-vector of common latent factors at time t, following the multivariate normal distribution:

$$z_t \sim \mathcal{N}(0, \Phi_t), \quad (2)$$

where 0 denotes the q-mean vector and Φ_t the diagonal covariance matrix of dimension $(q \times q)$ of the common latent factors z_t. The common variances (diagonal elements of Φ_t) follow generalized quadratic autoregressive conditionally heteroskedastic processes of order 1, GQARCH(1,1). In this case, the l-th common variance at time t is defined as follows:

$$\phi_{l,t} = \gamma_{0,l} + \gamma_{1,l} z_{l,t-1} + \gamma_{2,l} z_{l,t-1}^2 + \gamma_{3,l} \phi_{l,t-1} \quad (3)$$

Assuming that $\gamma_{1,l}, \gamma_{2,l} > 0$, the impact of a negative shock ($z_{l,t-1} < 0$) on the common volatility $\phi_{l,t}$ is lower than the impact of a positive shock ($z_{l,t-1} > 0$).

Lastly the p-vector of specific factors can be formulated using the multivariate normal distribution:

$$\nu_t \sim \mathcal{N}(\mu, \Sigma), \quad (4)$$

where μ denotes the mean vector of dimension p and Σ denotes the diagonal covariance matrix of the p specific factors.

To guarantee the common variance stationarity and positivity, some restrictions on the GQARCH parameters are needed, such as: $\gamma_{2,l} + \gamma_{3,l} < 1$, $\gamma_{0,l}, \gamma_{2,l}, \gamma_{3,l} > 0$ and $\gamma_{1,l}^2 \leq 4\gamma_{0,l}\gamma_{2,l}$, $\forall\, l = 1, \dots, q$.

To ensure the identification of the factor model (1), some other restrictions are needed, such as: $rank(\Gamma) = q$ and $p \geq q$. We assume also the non-correlation and the mutual independence of the factors z_t and ν_t. For more details on the identification problem, see Carnero (2004) and Saidane and Lavergne, (2011).

2.1 Inference of the latent factors structures

Because the common factors are unobserved, our model can be written as a dynamic state-space model with an observation equation:

[1] The opening price at the first trading day is denoted by $p_{k,0}$.

$$r_t = \mu + \Gamma z_t + \nu_t$$

and a transition equation:

$$z_t = 0 \cdot z_{t-1} + z_t,$$

where

$$\nu_t | r_{1:t-1}, z_{1:t-1} \sim \mathcal{N}(\mu, \Sigma)$$

and

$$z_t | r_{1:t-1}, z_{1:t-1} \sim \mathcal{N}(0, \Phi_t)$$

In this case $r_{1:t-1} = \{r_{t-1}, r_{t-2}, ...\}$ and $z_{1:t-1} = \{z_{t-1}, z_{t-2}, ...\}$, i.e. the information set $\mathcal{D}_{t-1}$ available at time $t-1$.

Hence the prediction equations are given by:

$$\mathbb{E}(z_t | \mathcal{D}_{t-1}) = z_{t|t-1} = 0$$

$$\mathbb{E}(r_t | \mathcal{D}_{t-1}) = r_{t|t-1} = \mu$$

and

$$Var(z_{l,t} | \mathcal{D}_{t-1}) = \phi_{l,t|t-1},$$

where

$$\phi_{l,t|t-1} = \gamma_{0,l} + \gamma_{1,l} z_{l,t-1|t-1} + \gamma_{2,l}\left(z_{l,t-1|t-1}^2 + \phi_{l,t-1|t-1}\right) + \gamma_{3,l}\phi_{l,t-1|t-2}$$

In the previous equation $\phi_{l,t|t-1}$ denotes the *l*-th diagonal element of $\Phi_{t|t-1}$ and the *l*-th diagonal element of $\Phi_{t-1|t-1}$ is given by:

$$\phi_{l,t-1|t-1} = Var(z_{l,t-1} | \mathcal{D}_{t-1}),$$

where the term $\phi_{l,t-1|t-1}$ comes from the fact that

$$E\left(z_{l,t-1}^2 | \mathcal{D}_{t-1}\right) = Var\left(z_{l,t-1} | \mathcal{D}_{t-1}\right) + E\left(z_{l,t-1} | \mathcal{D}_{t-1}\right)^2 = \phi_{l,t-1|t-1} + z_{l,t-1|t-1}^2$$

and

$$z_{l,t-1|t-1} = \mathbb{E}\left(z_{l,t-1} | \mathcal{D}_{t-1}\right)$$

Using the Kalman updating routine (See, Saidane and Lavergne, 2011), we update the mean and the variance estimates as follows:

$$z_{t|t} = z_{t|t-1} + \Phi_{t|t-1}\Gamma'\Omega_{t|t-1}^{-1}\left(r_t - \mu - \Gamma z_{t|t-1}\right)$$

and

$$\Phi_{t|t} = \Phi_{t|t-1} - \Phi_{t|t-1}\Gamma'\Omega_{t|t-1}^{-1}\Gamma\Phi_{t|t-1},$$

where

$$\Omega_{t|t-1} = \Gamma\Phi_{t|t-1}\Gamma' + \Sigma.$$

In this case smoothing is unnecessary, given the degenerate nature of the transition equation, so that $z_{t|T} = z_{t|t}$ and $\Phi_{t|T} = \Phi_{t|t}$.

2.2 The EM algorithm

To estimate the model parameters Θ, we consider an iterative approach using the Expectation Maximization (EM) algorithm (Dempster et al., 1977 and McLachlan and Krishnan, 2008) in conjunction with a Kalman filtering step for latent state estimation. At each iteration, our algorithm consists in two steps. In the E-step, we calculate the conditional expectation of the complete log-likelihood function with respect to the posterior probability of the latent variables (Z, S), given the current iteration's parameter values $\Theta^{(e)}$. In this case, the complete log-likelihood function can be written as:

$$\mathcal{L}(\Theta|r, Z) = -\frac{Tp}{2}\log 2\pi - \frac{1}{2}\sum_{t=1}^{T}\log|\Sigma|$$
$$-\frac{1}{2}\sum_{t=1}^{T} tr[\Sigma^{-1}(r_t - \mathrm{B}\tilde{r}_t)(r_t - \mathrm{B}\tilde{r}_t)'] - \frac{1}{2}\sum_{l=1}^{q}\left[\sum_{t=1}^{T}\log\phi_{l,t} + \sum_{t=1}^{T}\frac{z_{l,t}^2}{\phi_{l,t}}\right],$$

where $\tilde{r}_t' = [1|r_t']$ and $\mathrm{B} = [\mu|\Gamma]$ is the $p \times (q+1)$ matrix of "regression" parameters.

Then, in the M-step, we maximize the conditional expectation of the complete log-likelihood function (5), and update the estimates for the unknown parameters Θ.

$$Q\left(\Theta|\Theta^{(e)}\right) \simeq c - \frac{1}{2}\sum_{t=1}^{T}\log|\Sigma| - \frac{1}{2}\sum_{t=1}^{T} tr\left[\Sigma^{-1}\mathbb{E}\left((r_t - \mathrm{B}\tilde{r}_t)(r_t - \mathrm{B}\tilde{r}_t)'|r_{1:T}, \Theta^{(e)}\right)\right]$$
$$-\frac{1}{2}\sum_{l=1}^{q}\sum_{t=1}^{T}\mathbb{E}\left[\log\phi_{l,t} + \frac{z_{l,t}^2}{\phi_{l,t}}|r_{1:T}, \Theta^{(e)}\right] \qquad (5)$$

These iterations will be repeated until convergence is reached.

Given the nonlinearity of the relationships between the parameters of the common latent factor variances involved in the last component of equation (5), we need to maximize in a first time equation (5) with respect to the vector of specific means μ, the loadings matrix Γ and the covariance matrix of specific factors Σ. Thereafter, the common volatility parameters can be updated via numerical maximization.

The optimization of equation (5) with respect to the "regression" parameters matrix gives updated estimates for the specific means vector and the matrix of factor loadings:

$$\mathrm{B}^{(e+1)} = \left[\sum_{t=1}^{T} r_t\,\mathbb{E}\left(\tilde{r}_t'|r_{1:T}, \Theta^{(e)}\right)\right]\left[\sum_{t=1}^{T}\mathbb{E}\left(\tilde{r}_t\tilde{r}_t'|r_{1:T}, \Theta^{(e)}\right)\right]^{-1} \qquad (6)$$

Using these estimates, we can then estimate the specific covariance matrix as follows:

$$\Sigma^{(e+1)} = \frac{1}{T}\sum_{t=1}^{T}\mathbb{E}\left[(r_t - \mathrm{B}\tilde{r}_t)(r_t - \mathrm{B}\tilde{r}_t)'|r_{1:T}, \Theta^{(e)}\right] \qquad (7)$$

In this step, the conditional expectations in (6) and (7) can be obtained employing the sufficient statistics given by the Kalman filtering procedure in section 2.1.

We note here that the filtering algorithm produces approximate conditional expectations because the covariance matrix Φ_t is itself a function of the common latent factors. If we denote by $\tilde{r}_{t|t}^{(e)'} = \left(1\,, z_{t|t}^{(e)\prime}\right)$ the conditional expectation $\mathbb{E}\left(\tilde{r}_t{}'|r_{1:t}, \Theta^{(e)}\right)$ and $\Psi_{t|t}^{(e)}$ the conditional expectation $\mathbb{E}\left(\tilde{r}_t\tilde{r}_t{}'|r_{1:t}, \Theta^{(e)}\right)$, we obtain:

$$\Psi_{t|t}^{(e)} = \mathbb{E}\left[\begin{pmatrix} 1 & z_t{}' \\ z_t & z_t z_t{}' \end{pmatrix} |r_{1:t}, \Theta^{(e)}\right] = \begin{bmatrix} 1 & z_{t|t}^{(e)\prime} \\ z_{t|t}^{(e)} & \Phi_{t|t}^{(e)} + z_{t|t}^{(e)} z_{t|t}^{(e)\prime} \end{bmatrix}$$

By using this equation, we get the updated specific means and factor loadings as follows:

$$\mathrm{B}^{(e+1)} = \left[\sum_{t=1}^{T} r_t \tilde{r}_{t|t}^{(e)\prime}\right]\left[\sum_{t=1}^{T} \Psi_{\mathrm{t|t}}^{(\mathrm{e})}\right]^{-1}$$

and the updated specific covariance matrix as follows:

$$\Sigma^{(e+1)} = \frac{1}{T}\sum_{t=1}^{T}\left[r_t r_t' - \mathrm{B}^{(e+1)} \tilde{r}_{t|t}^{(e)} r_t{}'\right]$$

Following Harvey et al., (1992), we can approach the posterior distribution of the log-return series, given the updated estimates of μ, Γ and Σ as follows:

$$r_t|r_{1:t-1}, \sim \mathcal{N}\left[\mu, \Omega_{t|t-1}\right],$$

where

$$\Omega_{t|t-1} = \Gamma\Phi_{t|t-1}\Gamma' + \Sigma$$

and $\Phi_{t|t-1}$ is the conditional expectation of Φ_t, given the sequence of log-returns $r_{1:t-1}$, provided by the extended Kalman filtering procedure developed in section 2.1:

$$\Phi_{t|t-1} = diag\left[\phi_{l,t|t-1}\right]_{l=1,\dots,q}$$

Taking these approximations, we obtain after disregarding the initial conditions, the following approached log-likelihood function:

$$\mathcal{L}^* = c - \frac{1}{2}\sum_{t=1}^{T}\log\left|\Omega_{t|t-1}\right| - \frac{1}{2}\sum_{t=1}^{T}(r_t - \mu)'\Omega_{t|t-1}^{-1}(r_t - \mu) \qquad (8)$$

Following Demos and Sentana (1998), in a first step we disregard the last component of the auxiliary function (5). After that, we optimize the remaining components with respect to (μ, Γ and Σ) via the EM algorithm. In this stage, the parameters of the conditionally heteroskedastic component $\gamma = \{\gamma_0, \gamma_1, \gamma_2, \gamma_3\}$ will be left unchanged compared to their values of the previous iteration. In a second step, the approached log-likelihood function (8) will be maximized with respect to γ, given the estimates of μ, Γ

and Σ obtained in the first stage. To solve this optimization problem, we used in this step the NlcOptim R-package (see, Chen and Yin, 2019).

2.3 Forecasting

The expected mean of the predictive distribution of the LFVM model conditional on the information set at time t, $\mathcal{D}_t$ is given by:

$$\mathbb{E}(r_{t+1}|\mathcal{D}_t) = \mu_{t+1|t} = \mu \quad (9)$$

and the predictive covariance matrix can be written as follows:

$$Var(r_{t+1}|\mathcal{D}_t) = \Omega_{t+1|t} = \Sigma + \Gamma\Phi_{t+1|t}\Gamma' \quad (10)$$

Within this framework, adaptive forecasting and parameter adjustment processes are performed simultaneously. In this case, the cryptocurrency closing prices adjusted for splits at the end of each trading day are incorporated in the database. The parameters of the model will be then adjusted based on the most recent observed database and the updated common latent volatility predictions (the diagonal elements of the latent factor covariance matrix $\Phi_{t+1|t}$) will be computed as follows:

$$\begin{aligned}
\tilde{\phi}_{l,t+1|t} &= \gamma_{0,l} + \gamma_{1,l}\mathbb{E}\big(z_{l,t}|\mathcal{D}_t\big) + \gamma_{2,l}\mathbb{E}\big(z_{l,t}^2|\mathcal{D}_t\big) + \gamma_{3,l}\mathbb{E}\big(\phi_{l,t}|\mathcal{D}_t\big) \\
&= \gamma_{0,l} + \gamma_{1,l}z_{l,t|t} + \gamma_{2,l}z_{l,t|t}^2 + \gamma_{3,l}\phi_{l,t|t} \\
\tilde{\phi}_{l,t+2|t} &= \gamma_{0,l} + \gamma_{1,l}\mathbb{E}\big(z_{l,t+1}|\mathcal{D}_t\big) + \gamma_{2,l}\mathbb{E}\big(z_{l,t+1}^2|\mathcal{D}_t\big) + \gamma_{3,l}\mathbb{E}\big(\phi_{l,t+1}|\mathcal{D}_t\big) \\
&= \gamma_{0,l} + \big(\gamma_{1,l} + \gamma_{2,l}\big)\tilde{\phi}_{l,t+1|t} \\
&\vdots
\end{aligned}$$

and for forecasting horizons $h > 2$, we have:

$$\tilde{\phi}_{l,t+h|t} = \gamma_{0,l}\left[\sum_{j=0}^{h-2}\big(\gamma_{2,l} + \gamma_{3,l}\big)^j\right] + \big(\gamma_{2,l} + \gamma_{3,l}\big)^{h-1}\tilde{\phi}_{l,t+1|t}$$

under the stationarity condition $\big(\gamma_{2,l} + \gamma_{3,l} < 1, \forall\, l\big)$, we have also

$$\lim_{h\to\infty}\tilde{\phi}_{l,t+h|t} \simeq \frac{\gamma_{0,l}}{1 - \gamma_{2,l} - \gamma_{3,l}}$$

Given the predictions of the common latent factor variances, the predicted portfolio's covariance matrix can be obtained as follows:

$$\Omega_{t+h|t} = \Sigma + \Gamma\Phi_{t+h|t}\Gamma',$$

where

$$\Phi_{t+h|t} = diag\big[\phi_{l,t+h|t}\big]_{l=1,\dots,q}$$

3. Using the LFVM for cryptocurrencies prediction

In this empirical assessment, we implement the LFVM to evaluate its performance in analyzing the latent dynamic correlation structure among the log-returns of six major cryptocurrencies. The optimal specification obtained with the Bayesian information criterion, BIC (Schwarz, 1978) and other competing specifications will then be used to evaluate the forecasting ability of the proposed approach. All the results are obtained using the R programming environment for statistical computing (version 4.1).

3.1 Data presentation and summary

In this first application, we focus on the price indexes of six major cryptocurrencies, namely the Bitcoin (BTC), Ethereum (ETH), Litecoin (LTC), Monero (XMR), Binance Coin (BNB) and Waves currencies. Cryptocurrencies are subject to changes in price due to imbalance between supply and demand but do not have any natural mechanism that produces dividends and returns. For this reason we will assume in the following that their price can be modeled as a geometric random walk. Our dataset, downloaded from the "Coin Market Cap" website[2], covers the period from 01/01/2017 to 31/12/2021, includes 1250 daily log-returns for the cryptocurrencies expressed in terms of American dollars (USD).

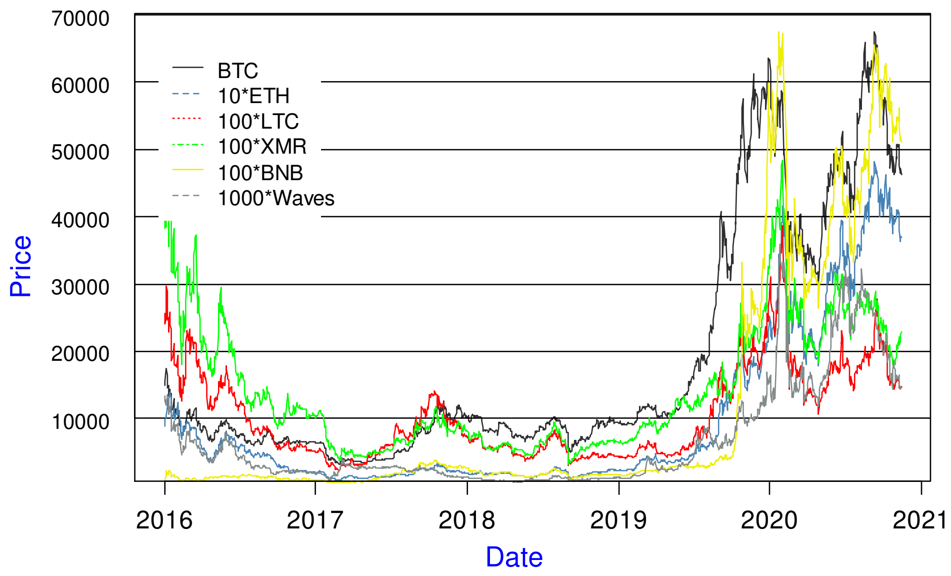

Figure 1: Time series of the daily closing prices of the different cryptocurrencies for the period from 1 January 2017, to 31 December 2021.

Figure 1 depicts the temporal path of the daily cryptocurrency prices from January 01, 2017 to December 31, 2021. In order to get comparisons, some prices have been adequately scaled. We can notice here the high volatility characterizing the crypto market and the phases of galloping price increases. The first big price increase wave started at the beginning of the second half of 2017, the big "bubble" that brought the Bitcoin's price to exceed 20,000 USD for the first time, a second "bubble" in mid-2019, and the most recent one has begun towards the end of 2020.

Figure 2 plots the evolution of the log-returns at closing for the different series, confirming the high volatility characterizing the six cryptocurrencies and showing the

[2] https://coinmarketcap.com/

presence of volatility clustering and persistence in crypto market during this period (high-volatility periods are followed by high-volatility and vice versa).

Note also that all the observed correlations between the different log-returns are greater than 0.5 and very high for the pairs BTC-ETH (0.805), ETH-LTC (0.820), BTC-XMR (0.752) and LTC-XMR (0.739), showing a strong degree of comovement between them, during both stability and crisis periods. In this case, the partial correlations between the different pairs of cryptocurrencies are not so obvious to interpret, suggesting that the dominance of the Bitcoin does not necessarily result in a unique commoving driver.

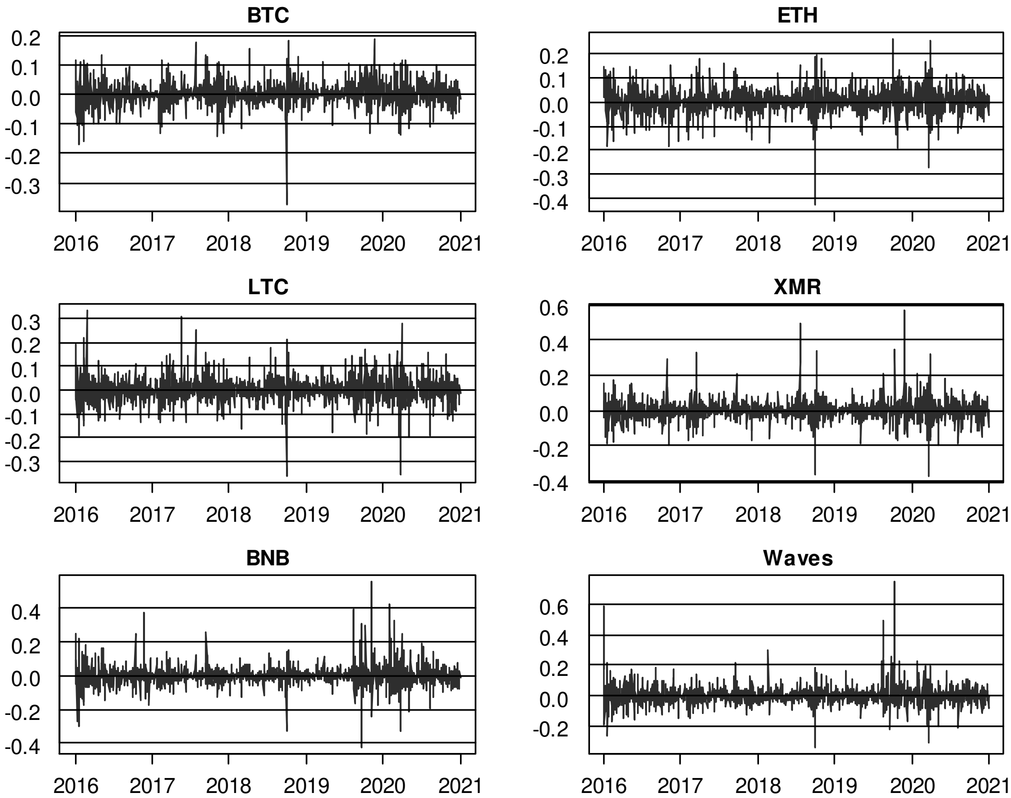

Figure 2: Daily log-returns of the different cryptocurrencies based on closing prices for the period from January 01, 2017, to December 31, 2021.

Table 1 gives some descriptive statistics of the data and reports the results of the D'Agostino, (1970) and Anscombe-Glynn, (1983) omnibus normality test. The results of the Jarque-Bera, (1980) normality test are also, given in this table. We note here that the Lagrange multiplier statistic consists in testing the kurtosis and skewness coefficients against their normal counterparts. It can be seen from the results that the log-returns are not normally distributed since the BTC, ETH and XMR returns exhibit significant negative skewness and those of the LTC, BNB and Waves currencies exhibits positive skewness with an excess kurtosis and a heavier tail, relative to a normal distribution for all the series during the full period.

Table 1: Summary statistics of the daily log-returns from 01/01/2017 to 31/12/2021.

Statistic	BTC	ETH	LTC	XMR	BNB	Waves
Mean	0.0016359	0.0024051	0.0011893	0.0011755	0.0046877	0.00223265
Max	0.1875	0.2595	0. 3372	0.4119	0.6976	0.5648
Median	0.00139	0.00110	0.00005	0.00213	0.00115	0.00071
Min	-0.3717	- 0.4235	-0.3618	-0.4138	-0.4190	-0.3856
Std. Dev.	0.0396	0.0511	0.0054	0.0538	0.0627	0.0662
D'Agost. test	-6.35634	-5.48774	1.501550	-4.2945	20.7260	13.8556
	(0.0000)	(0.0000)	(0.1332)	(0.0000)	(0.0000)	(0.0000)
A-Glyn. test	14.949	13.5028	13.6525	15.207	19.890	16.344
	(0.0000)	(0.0000)	(0.0000)	(0.0000)	(0.0000)	(0.0000)
LB. test	18.399	34.057	24.373	54.96	20.488	41.603
	(0.1041)	(0.0006)	(0.0180)	(0.0000)	(0.0584)	(0.0000)
J-Bera. test	3461	1927	2015.3	3824.6	33902	6444.6
	(0.0000)	(0.0000)	(0.0000)	(0.0000)	(0.0000)	(0.0000)
ARCH-LM test	642.83	528.72	553.69	601.24	586.14	567.32
	(0.0000)	(0.0000)	(0.0000)	(0.0000)	(0.0000)	(0.0000)

p-values of the different tests are indicated in brackets.

Finally, we note that the results of the ARCH-LM test (Engle, 1982) show a significant ARCH effect and the existence of volatility clustering phenomena in the log-return series. In this case, the empirical test statistics for the different series are higher than the LM-critical value at the 1% significance level (p-values < 0.01), which imply that a quadratic GARCH (1,1) specification could give more appropriate solutions for the time-varying volatility which cannot be captured through linear models.

3.2 An exploratory analysis of the latent structure of the data

In this exploratory analysis, the uncertainty associated with the number of common latent factors is firstly explored. With this objective, we have examined different specifications using 1, 2 and 3 (standard and conditionally heteroskedastic) latent factors. Following Saidane (2022a,b), the BIC criterion is used and the results have revealed that the optimal specification for the log-return dynamics is the one with two common conditionally heteroskedastic latent factors. The estimation results of this model are given in Table 2.

Table 2: Estimation results of the optimal LFVM model for the period 01/01/2017 - 31/12/2019.

Model parameters (1e-03)	*Currencies*					
	BTC	ETH	LTC	XMR	BNB	Waves
$\hat{\mu}$	2.3006	3.6886	1.4110	1.9141	4.3691	3.5670
$\hat{\Gamma}$	2.0344	2.6667	2.8139	2.4231	2.5746	2.3652
	0.0000	1.0579	1.9568	1.7648	1.5664	1.7752
$\hat{\Sigma}$	0.3706	0.4451	0.5696	0.9859	1.5801	2.7737
$\hat{\gamma}$	*Factor 1*	0.2014	0.1265	0.1034	0.5681	
	Factor 2	0.1672	0.1485	0.1257	0.6430	

On this same database we have implemented the dynamic variance-matrix discounting method (VD); the naïve forecasting method using the average of the available data; the mixture of probabilistic factor analyzers (MFA) and the Gaussian dynamic state-space model (SSM). The fitted models were, then used to predict the volatility of the different series $(\hat{\sigma}_{j,t}^2)$ for periods of five days. In order to compute the realized latent volatilities, we have used the naive variance estimator given by the following formula:

$$\begin{cases} \sigma_{i,t}^2 = \sum_{j=t}^{t+4} \left(r_{i,j} - \bar{r}_{i,t}\right)^2 \\ \bar{r}_{i,t} = \frac{1}{5}\sum_{j=t}^{t+4} r_{i,j} \end{cases}$$

In this application, we used a rolling estimation and prediction scheme. The first 750 log-returns were used to estimate the different specifications (as illustrated in Section 2). Thereafter, 5 predicted variances for the common latent factors were computed, as described in section 2.3. The weekly variance forecasts of the different series were also computed using the other competing models. Using the naive variance estimator, the realized volatility of this week was computed too. Then, the same procedure was repeated again after shifting the estimation windows one week towards the future.

In order to compare the forecasting ability of competing models, we employed the forecast encompassing test developed by Chong and Hendry (1986). Practical implementations of this test, including out-of-sample forecasting comparisons using financial data, can be found in Thompson et al., (2015), Saidane and Lavergne (2011) and Clements and Harvey (2006). The basic idea behind the forecasting encompassing test is straightforward: we say that model $\mathcal{M}_j$ is encompassed by model $\mathcal{M}_i$, if the last one can explain what $\mathcal{M}_j$ cannot explain, and the converse is not true. Thus, the prediction error from the correctly specified volatility model should not be significantly related to any other information available for the forecaster.

The encompassing tests consist of the following set of simple linear regressions:

$$\left(\sigma_{j,t}^2 - \hat{\sigma}_{j,t}^2\right) = \lambda_1 + \delta_{j,i}\hat{\sigma}_{i,t}^2 + \eta_t \quad (11)$$

$$\left(\sigma_{i,t}^2 - \hat{\sigma}_{i,t}^2\right) = \lambda_2 + \pi_{i,j}\hat{\sigma}_{j,t}^2 + \upsilon_t, \quad (12)$$

where $\left(\sigma_{j,t}^2 - \hat{\sigma}_{j,t}^2\right)$ and $\left(\sigma_{i,t}^2 - \hat{\sigma}_{i,t}^2\right)$ are the forecast errors and $\hat{\sigma}_{j,t}^2$, $\hat{\sigma}_{i,t}^2$ the forecasts obtained, respectively, from models $\mathcal{M}_j$ and $\mathcal{M}_i$ at time t and η_t and υ_t are random errors. Based on these regressions we test the significance of the parameters $\delta_{j,i}$ and $\pi_{i,j}$.

In this case, at some confidence level, if the hypothesis H_0: $\pi_{i,j} = 0$ is rejected in (12), but H_0: $\delta_{j,i} = 0$ is not rejected in (11), then model $\mathcal{M}_j$ encompasses $\mathcal{M}_i$. Inversely, if the hypothesis H_0: $\delta_{j,i} = 0$ is rejected in (11), but H_0: $\pi_{i,j} = 0$ is not rejected in (12), we say that model $\mathcal{M}_i$ encompasses $\mathcal{M}_j$. If H_0: $\delta_{j,i} = 0$ in (11) and H_0: $\pi_{i,j} = 0$ in (12) are both rejected, or not rejected we say that neither forecast encompasses the other.

Table 3: The forecast encompassing *p*-values for the BTC, ETH and LTC data on the period 01/01/2020 - 31/12/2021.

Currency	Forecast error $\left(\hat{\sigma}_{i,t}^2 - \hat{\sigma}_{j,t}^2\right)$ from ↓	Forecast $\hat{\sigma}_{i,t}^2$ from ↓				
		LFVM	VD	MFA	SSM	Naive
BTC	LFVM	NA	0.6712	0.2861	0.3127	0.8524
	VD	0.0267	NA	0.0371	0.0302	0.2108
	MFA	0.0186	0.1108	NA	0.0429	0.4211
	SSM	0.0401	0.6320	0.1705	NA	0.5327
	Naive	0.0115	0.1125	0.0462	0.0415	NA
ETH	LFVM	NA	0.7126	0.3307	0.3854	0.7920
	VD	0.0192	NA	0.0264	0.0298	0.4610
	MFA	0.0208	0.3861	NA	0.0725	0.2201
	SSM	0.0473	0.0842	0.1102	NA	0.5104
	Naive	0.0188	0.1091	0.0483	0.0437	NA
LTC	LFVM	NA	0.4831	0.4120	0.3662	0.8647
	VD	0.0313	NA	0.0542	0.0288	0.2132
	MFA	0.0242	0.3386	NA	0.0645	0.3873
	SSM	0.0256	0.2304	0.0771	NA	0.5117
	Naive	0.0101	0.1274	0.0357	0.0440	NA

In tables 3 and 4, we give the results of the encompassing tests. In these tables, the dependent (explained) variables $\left(\hat{\sigma}_{i,t}^2 - \hat{\sigma}_{j,t}^2\right)$ are listed in the second column and the independent (explanatory) variables $\hat{\sigma}_{l,t}^2$, are listed in the second row. The numbers in the entries of the tables denote the *p*-values of the different tests associated with the robust t-statistics computed on the regression coefficients $\delta_{j,i}$ and $\pi_{i,j}$. We note here that a *p*-value lower than 0.05 is viewed as evidence against the null hypothesis: the model listed in the second column cannot encompass the model listed in the second row.

Table 4: The forecast encompassing *p*-values for the XMR, BNB and Waves data on the period 01/01/2020 - 31/12/2021.

Currency	Forecast error $\left(\hat{\sigma}_{i,t}^2 - \hat{\sigma}_{j,t}^2\right)$ from ↓	Forecast $\hat{\sigma}_{l,t}^2$ from ↓				
		LFVM	VD	MFA	SSM	Naive
XMR	LFVM	NA	0.6678	0.3273	0.3577	0.5750
	VD	0.0305	NA	0.0424	0.0345	0.2411
	MFA	0.0213	0.1267	NA	0.0491	0.4817
	SSM	0.0459	0.5229	0.1950	NA	0.6091
	Naive	0.0131	0.1429	0.0528	0.0475	NA
BNB	LFVM	NA	0.4151	0.3783	0.4408	0.7053
	VD	0.0220	NA	0.0302	0.0341	0.5273
	MFA	0.0238	0.3416	NA	0.0529	0.2518
	SSM	0.0341	0.0963	0.1260	NA	0.5838
	Naive	0.0215	0.1079	0.0552	0.0499	NA
Waves	LFVM	NA	0.5526	0.4713	0.4189	0.6891
	VD	0.0358	NA	0.0620	0.0329	0.2053
	MFA	0.0277	0.3873	NA	0.0738	0.4430
	SSM	0.0293	0.2635	0.0882	NA	0.5853
	Naive	0.0115	0.1343	0.0408	0.0503	NA

From the results reported in these tables, we can see that the *p*-values of the regression models using forecast errors from the LFVM model are greater than the significance level 5% for all the cryptocurrencies. These results reveal that none of this model' forecast error can be explained by other models', which imply that the LFVM is not encompassed by any competing specification. On the other hand, we notice that the variance predictions given by this model explain significantly the prediction errors of the other models. These findings justify the superiority of the proposed LFVM compared to the other competing models in prediction accuracy.

At the significance level of 5%, these results show also that the MFA encompasses the dynamic variance discounting and the Naive forecasting methods for the BCT and ETH currencies. For the XMR and BNB, the variance discounting is encompassed by the MFA, and for the LTC and Waves currencies, the Naive forecasting method is encompassed by the MFA.

We note also that the SSM encompasses the MFA for the BCT and XMR currencies. It encompasses the variance discounting for all the currencies and the Naive forecasting method for all the currencies except the Waves. The SSM is never encompassed by the MFA, the variance discounting and the Naïve forecasting methods. Furthermore, the dynamic variance discounting and the Naïve forecasting methods neither encompasses the other at even the 10% significance level.

In conclusion, since the LFVM is not encompassed by any of the competing forecasts while every other model is encompassed at least once, we can say that the forecasting performance of our proposed approach is much better than that of other baseline methods.

4. Dynamic portfolio allocation strategies

In this paper, we assume that all transactions (short or long) are instantaneous and without any cost. In what follows we denote by $\mathcal{P}_{t+1}$ the p-vector of investment proportions in the different crypto assets obtained by the optimal one-step ahead predictive model at time t. These proportions are subject to the only constraint $\mathcal{P}_t{}'\mathbf{1} = 1$, where $\mathbf{1}$ is the $(p \times 1)$ column vector of ones, and the best model at time t is the one with the highest realized portfolio return $r_t^* = \mathcal{P}_t{}' r_t$ over the allocation period.

The Markowitz approach to portfolio allocation involves the general mean-variance optimization at each point of time. This framework requires estimates of the expected return of each cryptocurrency, as well as the predicted covariance matrix of returns. All these predictions may be obtained from our LFVM and from the other competing models.

For the implementation of our sequential strategy, the one-step ahead predictions of the mean vectors and covariance matrices of the log-return vectors r_t, denoted here by $\mu_{t+1|t}$ and $\Omega_{t+1|t}$ can be obtained from equations (9) and (10).

Our sequential optimization strategy seeks at each time t the minimization of the portfolio's one-step ahead variance for a target expected return m. In this situation, the optimal portfolio for the period $t+1$ will be selected as the one with the minimum predicted one-step ahead variance $\mathcal{P}_{t+1}{}'\Omega_{t+1|t}\mathcal{P}_{t+1}$ subject to a given expected return $\mathcal{P}_{t+1}{}'\mu_{t+1|t} = m$ and the condition that $\mathcal{P}_{t+1}{}'\mathbf{1} = 1$. The set of portfolios with the highest expected return for a given risk (variance) level is called the efficient frontier. We can demonstrate that the efficient frontier is the solution $\mathcal{P}_{t+1}^{(m)}$ that minimizes $\frac{1}{2}\mathcal{P}_{t+1}{}'\Omega_{t+1|t}\mathcal{P}_{t+1}$ over the constraint set, (Markowitz, 1959). The well known solution to this quadratic programming problem through Lagrange multipliers is given by the mean-variance efficient portfolio,

$$\mathcal{P}_{t+1}^{(m)} = \Omega_{t+1|t}^{-1}\left(a\mu_{t+1|t} + b\mathbf{1}\right),$$

where

$$a = \mathbf{1}'\Omega_{t+1|t}^{-1}e$$

and

$$b = \mu_{t+1|t}{}'\Omega_{t+1|t}^{-1}e$$

with

$$e = \frac{\left(\mathbf{1}m - \mu_{t+1|t}\right)}{d}$$

and

$$d = \left(\mathbf{1}'\Omega_{t+1|t}^{-1}\mathbf{1}\right)\left(\mu_{t+1|t}{}'\Omega_{t+1|t}^{-1}\mu_{t+1|t}\right) - \left(\mathbf{1}'\Omega_{t+1|t}^{-1}\mu_{t+1|t}\right)^2$$

Two other standard portfolio allocations can be derived in the same way. First, the strictly risk-averse allocation strategy which just depends only on the estimation of the variance-covariance matrix, namely,

$$\mathcal{P}_{t+1}^{(mv)} = \left(\mathbf{1}'\Omega_{t+1|t}^{-1}\mathbf{1}\right)^{-1}\Omega_{t+1|t}^{-1}\mathbf{1}$$

and second, the so called target-independent allocation strategy implemented on the boundary of the efficient frontier:

$$\mathcal{P}_{t+1}^{(me)} = \left(\mathbf{1}'\Omega_{t+1|t}^{-1}\mu_{t+1|t}\right)^{-1}\Omega_{t+1|t}^{-1}\mu_{t+1|t}$$

4.1 Special Portfolio Strategies

There are of course different varieties and extensions of the three basic strategies presented above as a result of including or removing constraints. For instance, the restriction that $\mathcal{P}_{t+1}{}'\mathbf{1} = 1$ forces the decision maker to constrain his short or long positions in the specified market. However, there are many situations when the optimal decision would be to take your money to the bank in, for example, high volatility situations. Consider then allocation strategies without any restrictions on the vector $\mathcal{P}_{t+1}$, allowing for short and long positions across the cryptocurrencies without regard to resources. This characterizes the practical working environment in the global investments in major financial institutions as reported by the previous work of Quintana and Putnam (1996) on discounting models. The mean efficient portfolio with expected return target m, under an unconstrained strategy is given by:

$$\mathcal{P}_{t+1}^{(*m)} = \lambda\Omega_{t+1|t}^{-1}\mu_{t+1|t},$$

where

$$\lambda = \frac{m}{\left(\mu_{t+1|t}{}'\Omega_{t+1|t}^{-1}\mu_{t+1|t}\right)}$$

A different situation arises in the implementation of portfolios in higher dimension which usually result in extreme weights on particular assets. A traditional strategy in these cases is to introduce upper and lower constraints in the optimization problem, $l_{i,t} < a_{i,t} < u_{i,t}$. Typical choices of the bounds are $l_{i,t} = 0$ reflecting the fact that no short sales are allowed and a constant upper bound $u_{i,t} = u_0$. Consequently, the higher level of u_0 the more aggressive the portfolio in the sense of the few number of securities held and the higher tracking error of the portfolio. The focus in this paper is on the four basic portfolio strategies: the mean-variance efficient, the target independent, the strictly risk-averse allocation and the unconstrained mean efficient portfolio with expected return target m. These strategies will be used in the next paragraph mainly for model comparisons in the crypto portfolio allocation example.

4.2 Dynamic Portfolio Comparisons for Cryptocurrencies

Following the approaches by Levy and Lopes (2021a), Leon and Reveiz (2010), Aguilar and West (2000) and Quintana and Putnam (1996), model comparisons are performed with a clear focus on the one-step ahead predictive performance of our latent factor volatility model in the context of sequential portfolio allocations. Our approach is able to sequentially update the model parameters and learn the time-varying volatilities. Levy and Lopes (2021b) have suggested a similar approach, using a dynamic risk factor model, to scale multivariate return volatility predictions up to high-dimensions.

The comparisons are focused here on the predictive accuracy of our model and the other competing models. All the models are fitted to the daily log-returns of the BTC, ETH, LTC, XMR, BNB and Waves currencies. In a first time, we divided our dataset into training set and prediction set. The training, set contains 750 observations (the log-returns of the different cryptocurrencies over the period 01/01/2017-31/12/2019). Then, we used the different allocation strategies to evaluate the sequential (one-step ahead) predictive performance of our model on the remaining 500 observations covering the period 01/01/2020-31/12/2021. The performance of our methodology (in terms of cumulative financial returns) is evaluated here by using the one-day rolling window method with a window size of 750 trading days (see Saidane, 2022a).

In order to compare the forecasting performance of the different models, Figure 3 graphs the paths of the cumulative returns, over the prediction set period, given by the weights of the different sequential allocation strategies, using the optimal LFVM, with two conditionally heteroskedastic common latent factors; the dynamic variance-matrix discounting method with the optimal discounting coefficient $\alpha = 0.95$; the optimal MFA, with two common standard factors and two mixture components and the optimal dynamic SSM, with two latent state variables. In this figure, each panel corresponds to a specific investment strategy: the constrained mean-variance efficient portfolio $\mathcal{P}_t^{(m)}$ and the target-independent allocation $\mathcal{P}_t^{(me)}$ strategy, with the expected target daily return $m = 0.002$ (in the top left and top right panels). The strictly risk-averse allocation strategy $\mathcal{P}_t^{(mv)}$ and the mean efficient unconstrained portfolio $\mathcal{P}_t^{(*m)}$ with the expected target daily return $m = 0.002$ (in the bottom left and bottom right panels), respectively.

As can now be seen from Figure 3, the optimal time-varying volatility portfolio model clearly dominates (in terms of cumulative returns) all the other competing models both in the case of constrained or unconstrained sequential allocation strategies.

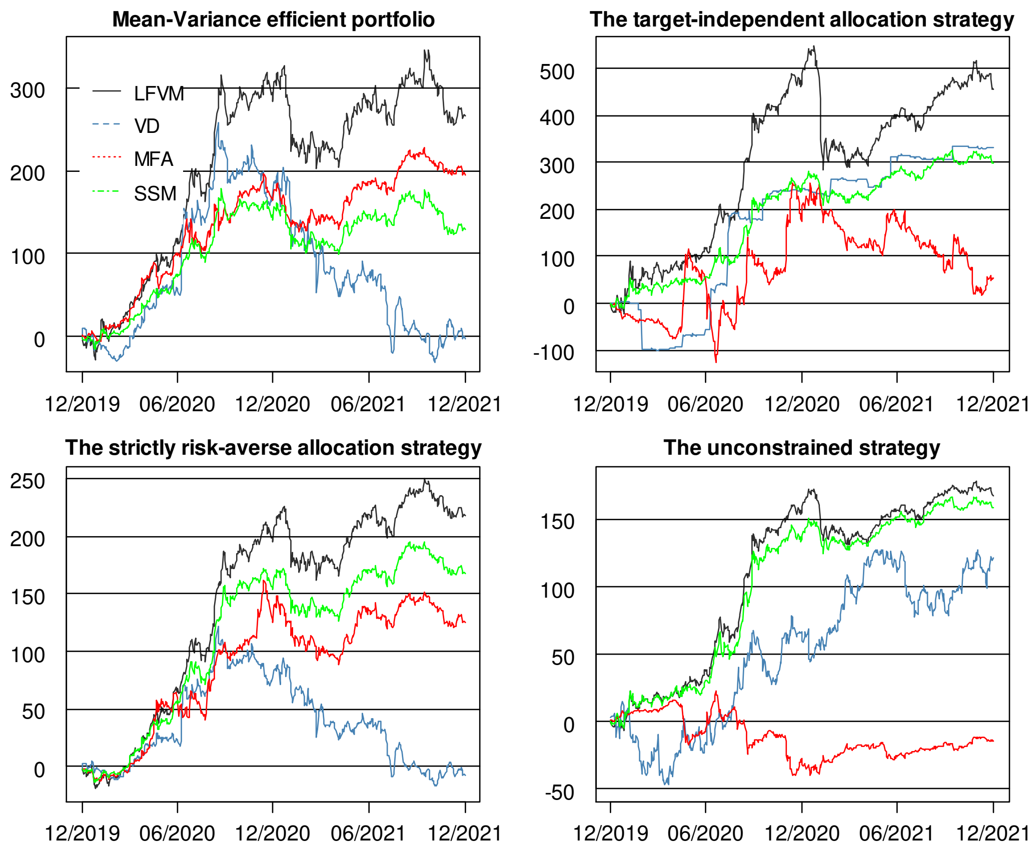

Figure 3: Cumulative returns under different dynamic portfolios, expressed in percentage terms (100 times their real values).

From this figure and the results of the encompassing tests presented in the previous section, we can conclude that the changes in volatility are better captured by the LFVM. The second ranked model is the dynamic SSM. These models behave closely the same in the computation of portfolio weights. They proceed to distinctly dominate all the other competing models in terms of cumulative returns for the different strategies, except in the case of the constrained optimal mean-variance allocation strategy where the MFA dominates the SSM.

In the case of the unconstrained allocation strategy, we can see again from Figure 3 a clear similarity in portfolio performance between the LFVM and the SSM. The main differences appear during high or increasing volatility periods, where the LFVM can markedly capitalize in terms of short-term gains compared to the dynamic SSM. The responsiveness of the conditionally heteroskedastic latent factor model leads in the short term to marked fluctuations in the crypto portfolio weights that the unconstrained strategies can significantly capitalize on, which can, thereafter, affect persistently the global cumulative returns.

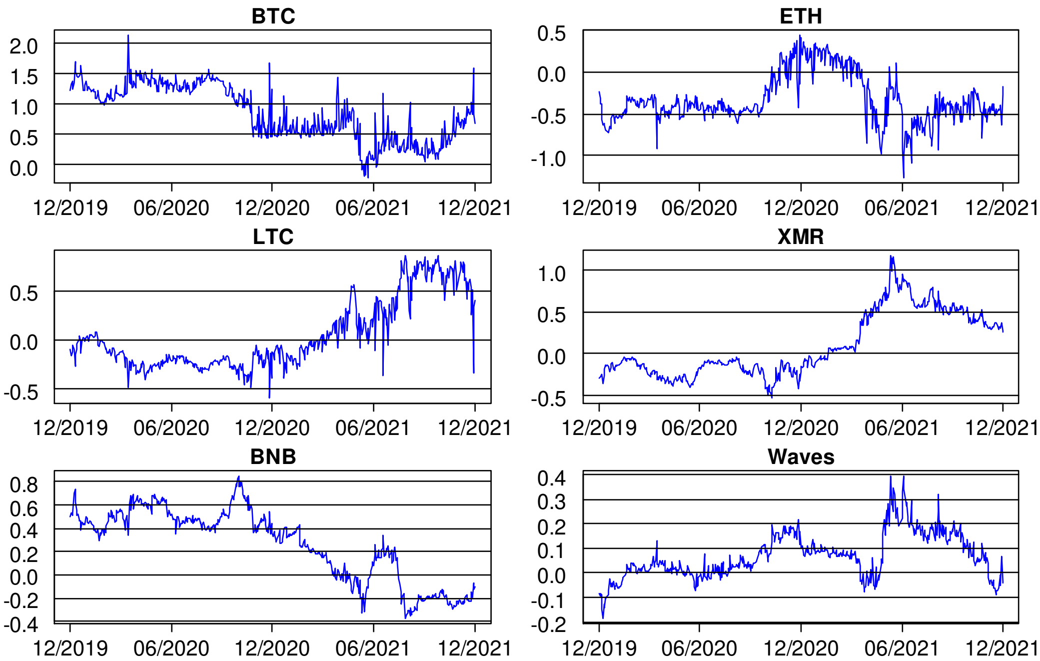

Figure 4: Dynamic weights $\mathcal{P}_t^{(m)}$ for the mean-variance efficient portfolio using the optimal LFVM.

In figures 4-7, we depict the weight trajectories of the different sequential allocation strategies, using only the optimal LFVM, with the expected target daily return $m = 0.002$ for the constrained and unconstrained mean-variance efficient portfolios. At each point of time, the plotted values are the relative weights of the different cryptocurrencies in the portfolio. The relative weight is the real value of the coefficient multiplied by 100 and divided by the sum $\mathbf{1}'\mathcal{P}_t$. These figures permit to compare directly the unconstrained weights with those given by the constrained allocation strategies, where the relative values coincide with the real ones.

We can see here the marked fluctuations in the portfolio structures as a response to the structural changes in volatility dynamics during the entire period. These fluctuations have been translated into a long-term persistence effect on the cumulative returns as shown in Figure 3.

It can be seen from Figure 4 that the allocations for the efficient constrained mean-variance strategy have been completely and quickly shifted to long positions on the LTC and the greatly associate XMR, while simultaneously taking quite completely short positions on the BNB and ETH currencies. We note here that, the first element of the vector μ is always positive, implying a positive expected return on the BTC around the end of 2019. This is reflected in the portfolios across the time period up to the end of 2021 through positive portfolio weights on the BTC; that is, the portfolios are long on the Bitcoin (characterized on average by low idiosyncratic risk during this period).

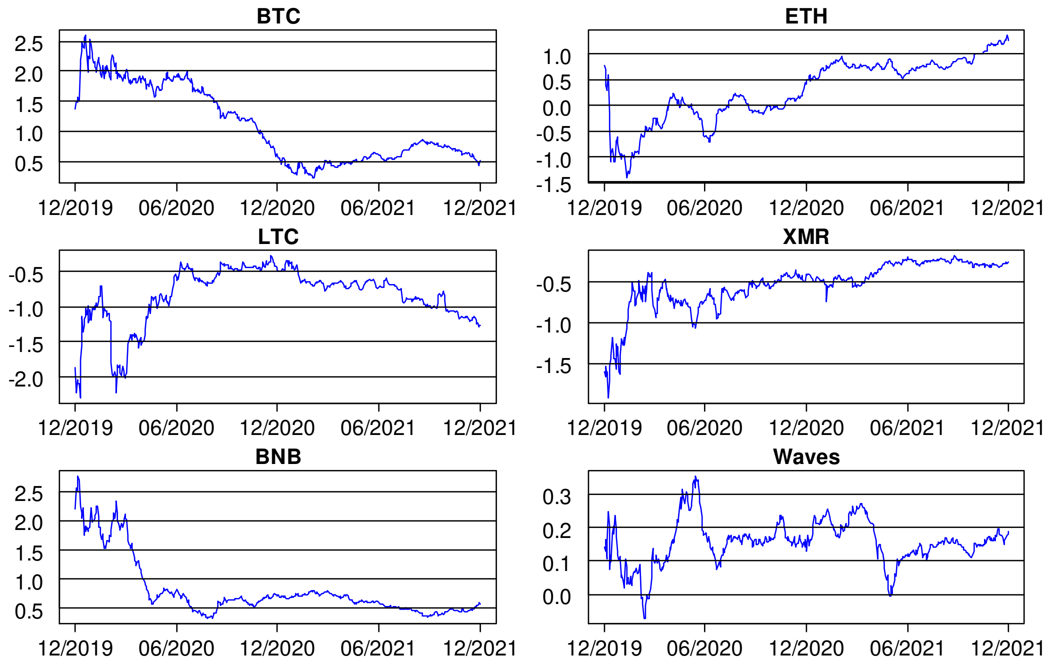

Figure 5: Dynamic weights $\mathcal{P}_t^{(me)}$ for the target-independent allocation derived at the boundary of the mean-variance efficient frontier using the optimal LFVM.

Figure 5 in connection with the long positions on BTC driven by the positive element of the mean vector μ, shows that, both constrained and the target-independent allocation derived at the boundary of the mean-variance efficient frontier portfolios adopt corresponding short positions on the LTC and ETH, and the portfolio weights on BTC and the pair (LTC,ETH) essentially offset each other.

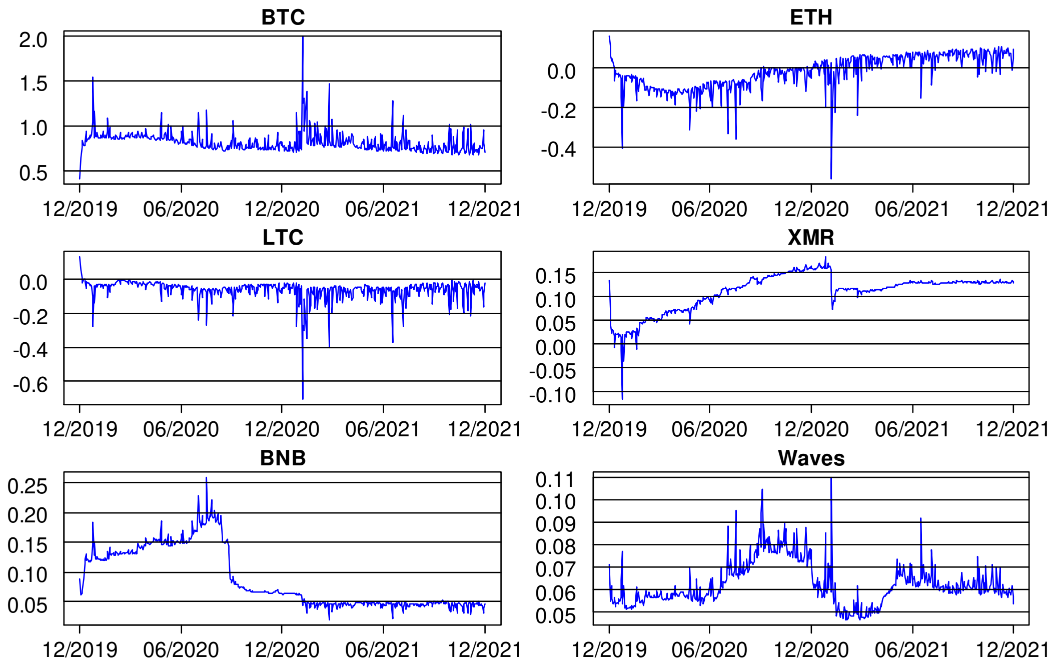

Figure 6: Dynamic weights $\mathcal{P}_t^{(mv)}$ for the strictly risk-averse minimum variance portfolio using the optimal LFVM.

From Figure 6, it can be noted that one of the most remarkable features of the portfolio weights paths given by the strictly risk-averse minimum variance strategy, is the very low weights associated to the LTC and Waves currencies during most of the study period. The components of the mean vector μ indicate, as is expected on economic grounds, an average return very close to zero for the Waves currency. Furthermore, we note that during the periods of very high idiosyncratic risk, the LTC weights tend to zero, which reflects an increase in the risk aversion index associated with this currency.

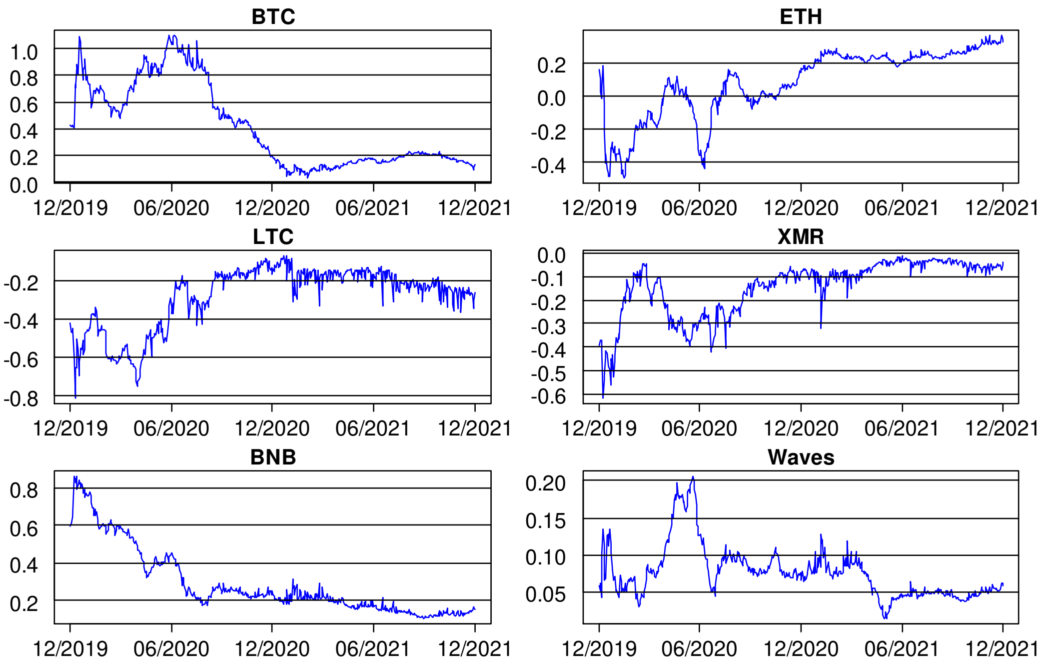

Figure 7: Dynamic weights $\mathcal{P}_t^{(*m)}$ for the mean efficient portfolio with expected return target $m = 0.002$, under an unconstrained strategy, using the optimal LFVM.

Comparison of figures 5 and 7 shows almost identical trajectories for the portfolio weights given by the target-independent allocation strategy and those given by the unconstrained strategy. We note here, as evidenced by the total investment $\mathbf{1}'\mathcal{P}_t^{(*m)}$ trajectories given in Figure 8, that the unconstrained strategies adopt overall long positions during the study period. This is highly affected by the positive mean and the resulting long positions for the BTC, BNB and Waves currencies reflect the response of the portfolio to the generally low volatility levels where compared to the target mean return, during the study period.

From Figure 8, we can clearly observe the relatively high fluctuations characterizing the temporal path of the sum $\mathbf{1}'\mathcal{P}_t^{(*m)}$ for the LFVM, during high volatility periods. It can be seen also from this figure that the total investment is decreased significantly during 2021: the considerable changes in volatility led to anticipate high levels of risk and as a result, the total amount invested in the market diminished significantly.

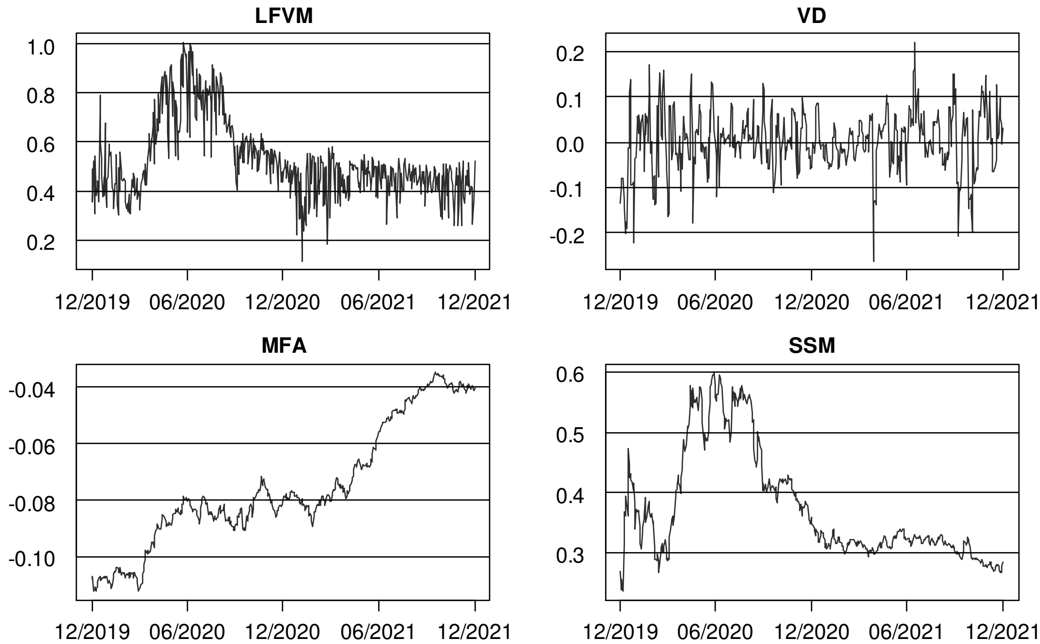

Figure 8: Total investments $\mathbf{1}'\mathcal{P}_t^{(*m)}$ with $m = 0.002$ in the unconstrained portfolios.

We note finally that, during the study period, while the dynamic SSM gives cumulative returns more or less close to those obtained by the LFVM, the portfolio weights obtained using the time-varying volatility structure are relatively more stationary over time. It is interesting to note also that the LFVM takes into account the time-varying cross-correlations between the cryptocurrency log-returns and gives more stationary portfolio's weight trajectories than those given by all the other competing models.

5. Conclusion

Asset allocation in a high dimensional mean-variance framework require a precise estimation of the covariance matrix of the portfolio's returns. The aim of this paper is to develop a quick and flexible multivariate conditionally heteroskedastic framework for price dynamics in order to make better predictions for dynamic crypto portfolio allocation.

Our studies demonstrate the feasibility of sequential predictions of the future volatility patterns based on the proposed conditionally heteroskedastic latent factor model. These predictions are computationally accessible with moderate computational resources, and our results showed that satisfactory predictions could be achieved for different forecasting horizons with high-dimensional time series and several factors. Currently we are working on the possibility to extend our model by relaxing the basic assumption of intertemporal stability of the portfolio's correlation structure, and the use of a Markov switching latent factorial approach for online crypto portfolio allocation. The example here supports the potential use of the proposed latent factor volatility model in the context of crypto-market research, where a conditionally heteroskedastic specification, taking into account the time-varying covariance structure, can improve the prediction performance and the portfolio decision making process, particularly in the case of constrained mean-variance allocation strategies. In the context of the unconstrained allocation strategies, the dynamic Gaussian state space model seems to works well, even, if it is finally dominated by the latent factor volatility model in terms of cumulative returns.

We think strongly that in the longer-term forecasting horizons and in more general models, taking volatility clustering into account and allowing for the possibility of regime changes in the intra-portfolio's latent correlation structure the dominance of the factorial approach will be much clearer. In this specification, which constitutes our future research, we will combine following Saidane and Lavergne (2007, 2009), conditionally heteroskedastic latent factor models with nonhomogeneous hidden Markov models, by relaxing the assumptions of constancy of the transition probabilities. We can also incorporate dynamic regressions on relative interest rates, energy prices and other possibly econometric indicators in the model. This can provide a more tractable way to handle heteroskedasticity and latent spatial-correlations in a multivariate framework, and can thereafter yield more accurate forecasts for crypto portfolio allocation, especially during crisis periods.

Acknowledgements

We would like to thank the editor and the reviewers for their constructive, careful and helpful feedback.

References

1. Aguilar, O., and West, M. (2000). Bayesian Dynamic Factor Models and Portfolio Allocation. *Journal of Business & Economic Statistics*, 18 (3), pp. 338-357.
2. Anscombe, F.J., Glynn, W.J., (1983). Distribution of kurtosis statistic for normal statistics. *Biometrika*, 70 (1), pp. 227-234.
3. Carnero, M.A., (2004). Persistence and Kurtosis in GARCH and Stochastic Volatility Models. *Journal of Financial Econometrics*, 2 (2), pp. 319-342.
4. Chen, X., and Yin, X. (2019). Solve Nonlinear Optimization with Nonlinear Constraints, Version 0.6. [online] https://cran.r-project.org/web/packages/NlcOptim/NlcOptim.pdf
5. Chong, Y.Y. and Hendry, D.F. (1986). Econometric evaluation of linear macroeconomics models. *Review of Economics Studies*, 53, pp. 671-690.
6. Clements, M. P. and Harvey, D. I. (2006). Forecast Encompassing Tests and Probability Forecasts. *Journal of Applied Econometrics*, 25 (6), pp.1028-1062.
7. D'Agostino, R.B., (1970). Transformation to Normality of the Null Distribution of G1. *Biometrika*, 57 (3), pp. 679-681.
8. Dempster, A.P., Laird, N.M. and Rubin, D.B. (1977) 'Maximum Likelihood from Incomplete Data via the EM Algorithm. *Journal of the Royal Statistical Society, Series B*, 39 (1), pp 1-38.

9. Engle, R. F. (1982). Autoregressive conditional heteroscedasticity with estimates of the variance of United Kingdom inflation. *Econometrica*, 50 (4), pp. 987-1007.
10. Harvey, A., Ruiz, E. and Sentana, E. (1992). Unobserved component time series models with ARCH disturbances. *Journal of Econometrics*, 52 (1-2), pp. 129-157.
11. Jarque, C.M., and Bera, A.K., (1980). Efficient test for normality, homoscedasticity and serial independence of residuals. *Economic Letters*, 6 (3), pp. 255-259.
12. Leon, C., and Reveiz, A. (2010). Portfolio optimization and long-term dependence. Banco de la Republica Working Paper No. 602.

    [online] https://papers.ssrn.com/sol3/papers.cfm?abstract_id=1686115
13. Levy, B. P., and Lopes, H. F. (2021a). Dynamic Ordering Learning in Multivariate Forecasting. arXiv preprint. [online] https://arxiv.org/pdf/2101.04164.pdf
14. Levy, B. P., and Lopes, H. F. (2021b). Dynamic Portfolio Allocation in High Dimensions using Sparse Risk Factors. arXiv preprint. [online] https://arxiv.org/pdf/2105.06584.pdf
15. Markowitz, H. M. (1959). Portfolio Selection: Efficient Diversification of Investments. New York: John Wiley and Sons.
16. McLachlan, G., and Krishnan, T. (2008). The EM Algorithm and Extensions, 2nd Edition. John Wiley and Sons, Inc., Hoboken, New Jersey, USA.
17. Mosbahi, M. N., Saidane, M., and Messabeb, S. (2017). Mixture of Probabilistic Factor Analyzers for Market Risk Measurement: Empirical Evidence from the Tunisian Foreign Exchange Market. *Risk governance and control: financial markets & institutions*, 7(2), pp. 158-169.
18. Putnam. B. W., and Quintana, J. M. (1994). New Bayesian Statistical Approaches to Estimating and Evaluating Models of Exchange Rates Determination. In Proceedings of the Section on Bayesian Statistical Science, American Statistical Association, pp. 232-237.
19. Quintana, J. M., and Putnam B. M. (1996). Debating Currency Markets Efficiency Using Multiple-Factor Models. In Proceedings of the Section on Bayesian Statistical Science, American Statistical Association, pp. 55-60.
20. Saidane, M. (2022a). Switching latent factor value-at-risk models for conditionally heteroskedastic portfolios: A comparative approach. *Communications in Statistics: Case Studies, Data Analysis and Applications*, 8 (2), pp. 282-307.
21. Saidane, M. (2022b). A New Viterbi-Based Decoding Strategy for Market Risk Tracking: an Application to the Tunisian Foreign Debt Portfolio During 2010–2012. *Statistika: Statistics and Economy Journal*, 102 (4), pp. 454-470.
22. Saidane, M., (2019). Forecasting Portfolio-Value-at-Risk with Mixed Factorial Hidden Markov Models. *Croatian Operational Research Review*, 10 (2), pp. 241-255.
23. Saidane, M. (2017). A Monte-Carlo-based Latent Factor Modeling Approach with Time-Varying Volatility for Value-at-Risk Estimation: Case of the Tunisian

Foreign Exchange Market. *Industrial Engineering & Management Systems*, 16 (3), pp. 400-414.

24. Saidane, M., and Lavergne, C., (2011). Can the GQARCH Latent Factor Model Improve the Prediction Performance of Multivariate Financial Time Series? *American Journal of Mathematical and Management Sciences*, 31 (1-2), pp. 73-116.
25. Saidane, M., and Lavergne, C., (2009). Optimal Prediction with Conditionally Heteroskedastic Factor Analysed Hidden Markov Models. *Computational Economics*, 34 (4), pp. 323-364.
26. Saidane, M., Lavergne, C. (2007). Conditionally heteroscedastic factorial HMMs for Time Series in Finance. *Applied Stochastic Models in Business and Industry*, 23 (6), pp. 503-529.
27. Saidane, M. (2006). Modèles à Facteurs Conditionnellement Hétéroscédastiques et à Structure Markovienne Cachée pour les Séries Financières. [Doctoral dissertation, Université Montpellier II - Sciences et Techniques du Languedoc]. http://tel.archives-ouvertes.fr/tel-00089558.
28. Schwarz, G. (1978). Estimating the dimension of a model. *The Annals of Statistics*, 6 (2), pp. 461-464.
29. Thompson, K., Eyden, R. and Gupta, R. (2015). Testing the Out-of-Sample Forecasting Ability of a Financial Conditions Index for South Africa. *Emerging Markets Finance and Trade*, 51 (3), pp. 486-501.